Mon. Not. R. Astron. Soc. **000**, 000–000 (0000) Printed 3 November 2004 (MN LaTeX style file v2.2)

Radiative feedback from quasars and the growth of massive black holes in stellar spheroids

S. Yu. Sazonov[1,2⋆], J. P. Ostriker[3], L. Ciotti[4], and R. A. Sunyaev[1,2]
[1] *Max-Planck-Institut für Astrophysik, Karl-Schwarzschild-Str. 1, 85740 Garching bei München, Germany*
[2] *Space Research Institute, Russian Academy of Sciences, Profsoyuznaya 84/32, 117997 Moscow, Russia*
[3] *Institute of Astronomy, Madingley Road, CB3 0HA Cambridge*
[4] *Department of Astronomy, University of Bologna, via Ranzani 1, I-40127 Bologna, Italy*

arXiv:astro-ph/0411086 v1 3 Nov 2004

3 November 2004

ABSTRACT
We discuss the importance of feedback via photoionization and Compton heating on the co-evolution of massive black holes (MBHs) at the center of spheroidal galaxies and their stellar and gaseous components. We first assess the energetics of the radiative feedback from a typical quasar on the ambient interstellar medium. We then demonstrate that the observed $M_{\rm BH}$–σ relation could be established following the conversion of most of the gas of an elliptical progenitor into stars, specifically when the gas-to-stars mass ratio in the central regions has dropped to a low level ∼0.01 or less, so that gas cooling is no longer able to keep up with the radiative heating by the growing central MBH. A considerable amount of the remaining gas will be expelled and both MBH accretion and star formation will proceed at significantly reduced rates thereafter, in agreement with observations of present day ellipticals. We find further support for this scenario by evolving over an equivalent Hubble time a simple, physically based toy model that additionally takes into account the mass and energy return for the spheroid evolving stellar population, a physical ingredient often neglected in similar approaches.

Key words: galaxies: active – galaxies: evolution – quasars: general.

1 INTRODUCTION

Elliptical galaxies are, with few exceptions, poor with respect to interstellar gas (e.g. O'Sullivan et al. 2001). Also, elliptical galaxies invariably contain central massive black holes (MBHs), and there exists a tight relationship between the characteristic stellar velocity dispersion σ and the black hole mass $M_{\rm BH}$ (Ferrarese & Merritt 2000; Tremaine et al. 2002), and between $M_{\rm BH}$ and the host spheroid mass in stars, M_* (Magorrian et al. 1998). Are these two facts related? Here we focus on a scenario in which the mass of the central MBH grows within gas rich elliptical progenitors until star formation has reduced the gas fraction in the central regions to of order 1 per cent of the stellar mass. Then radiative feedback, during episodes when the luminosity from the central MBH approaches its Eddington limit, heats and drives much of the remaining gas out of the galaxy, limiting both future growth of the MBH and future star formation to low levels.

We show that for a typical quasar spectral energy distribution (SED) the limit on the central MBH produced by this argument coincides accurately with the observed $M_{\rm BH}$-σ relation and we predict that the observed power law should break down below $10^4 M_\odot$ and above a few $10^9 M_\odot$. In our calculations, we adopt the average quasar SED derived by Sazonov et al. (2004, hereafter SOS) from cosmic background radiation fields supplemented by information from individual objects. Of key importance is that the UV and high energy radiation from *a typical quasar can photoionize and heat a low density gas up to an equilibrium Compton temperature ($T_{\rm C} \approx 2\times10^7$ K) that exceeds the virial temperatures of giant ellipticals*; the radiative effects on cluster gas are expected to be minimal (e.g. Ciotti, Ostriker & Pellegrini 2004) but the effects on gas within the host galaxy can be substantial. We note that the present paper is complementary to those by Ciotti & Ostriker (1997, 2001, hereafter CO97,01) in that, while it does not attempt to model the complex flaring behavior of an accreting MBH with an efficient hydrodynamical code, it does do a far more precise job of specifying the input spectrum and the detailed atomic physics required to understand the interaction between that spectrum and the ambient interstellar gas in elliptical galaxies.

The evolutionary scenario considered could explain sev-

⋆ E-mail: sazonov@mpa-garching.mpg.de

eral key observational facts. First, that giant ellipticals are old – they end their period of star formation early in cosmic time, since the radiative output from the central MBHs limits (in cooperation with the energetic input due to star formation) the gas content to be at levels for which ongoing star formation is minimal. Secondly, gas rich, actively star forming galaxies at redshift $z \sim 3$, including Lyman Break Galaxies and bright submillimeter SCUBA galaxies, generally exhibit only moderate active galactic nucleus (AGN) activity (Steidel et al. 2002; Alexander et al. 2003; Lehmer et al. 2004), indicating that their central MBHs are still growing. This suggests that the formation of a spheroid probably closely preceeds a quasar shining phase, which finds further support in spectroscopic observations showing that quasars live in a metal-enriched environment (e.g. Hamann & Ferland 1999). The redshift evolution of the quasar emissivity and of the star formation history in spheroids is thus expected to be roughly parallel since $z \sim 3$, which also is consistent with observations (e.g. Haiman et al. 2004; Heckman et al. 2004).

We note that many authors have already recognized the importance of feedback as a key ingredient of the mutual MBH and galaxy evolution (among them Binney & Tabor 1995; CO97; Silk & Rees 1998; Fabian 1999; CO01; Burkert & Silk 2001; Ciotti & van Albada 2001; Granato et al. 2001; Cavaliere & Vittorini 2002; King 2003; Wyithe & Loeb 2003; Haiman et al. 2004; Granato et al. 2004; Murray et al. 2004; Springel, Di Matteo & Hernquist 2004). What is new about this work is the stress on one component of the problem that has had relatively little attention – the *radiative output* of the central MBH.

We emphasize that the radiative output is not the only, nor even necessarily the dominant mechanism whereby feedback from accretion onto central MBHs can heat gas in elliptical galaxies. Binney & Tabor (1995) have stressed that the mechanical input from radio jets will also provide a significant source of energy, and much detailed work has been performed to follow up this suggestion. Strong evidence has accumulated over recent years that the radiative losses of hot gas in the 100 kpc-scale cores of galaxy clusters may be counteracted by the mechanical input from the central giant elliptical galaxies, which usually host a low luminosity AGN (e.g. Churazov et al. 2002). It is however not obvious that all AGNs, and in particular luminous quasars, produce radio jets, whereas all do appear to produce high energy radiation. In any case, the two mechanisms are complementary, and in this paper we are exploring only the radiative feedback. Given what we now know about the prevalence of MBHs in ellipticals, the tight relationship between the MBH mass and stellar mass, and the known efficiency for converting accreted mass into electromagnetic output with a specific spectrum, the consequence of radiative feedback can now be estimated with reasonable accuracy, more easily than can be acheived for the mechanical energy feedback.

This paper is organized as follows. In Section 2.1 we investigate the possibility of radiatively preheating a spherical accretion flow within 1–100 pc from a MBH. In Section 2.2 we assess the conditions for a significant heating of interstellar gas at larger distances from the central quasar. In Section 3 we propose that radiative feedback could be a key factor leading to the observed $M_{\rm BH}$–σ relation. In Section 4 we elaborate on this idea in the context of the MBH–galaxy co-evolution, using a simple, but physically motivated, one-zone model.

2 ENERGETICS OF THE RADIATIVE FEEDBACK

Radiative feedback from accretion onto a MBH can affect the accretion flow within the MBH sphere of influence, i.e. in the central 1–100 pc of the host galaxy [see equations (14) and (16)], as well as the interstellar gas at larger distances. Adopting the average quasar SED from SOS, we consider the effects arising in the former and later case in Section 2.1 and 2.2, respectively. We note that significant feedback effects are expected only when the luminosity L of the central MBH approaches the Eddington luminosity

$$L_{\rm Edd} = 1.3 \times 10^{46} \frac{M_{\rm BH}}{10^8 M_\odot} \,{\rm erg\,s^{-1}}, \tag{1}$$

hence our use of a SED typical of quasars throughout.

2.1 Preheating of a spherical accreting flow onto a MBH

Using hydrodynamical simulations and fiducial quasar SEDs, CO01 demonstrated that accretion of gas onto the central MBHs in elliptical galaxies cannot proceed stably at sub-Eddington rates if the mass-to-radiation conversion efficiency ϵ ($\equiv \Delta E_\gamma/\Delta mc^2$) is high (0.1), as is characteristic of quasars. During high luminosity episodes, the high energy radiation, primarily X-rays, from the MBH unbinds the accreting gas through Compton heating, which temporarily leads to a decrease in the mass inflow rate and consequently in the central luminosity. The SEDs utilized by CO01 covered a fair range, in general corresponding to a high Compton temperature. Our aim here is to verify whether the conclusions remain unaltered for the average quasar SED once photoionization is fully taken into account. We note that our treatment below is similar to previous semi-analytic studies of preheating of quasi-spherical accreting gas flows (e.g. Cowie et al. 1978; Krolik & London 1983; Park & Ostriker 1999).

SOS (see their fig. 5) computed for the average quasar SED the equilibrium temperature $T_{\rm eq}$ of gas of cosmic chemical composition as a function of the "ionization" parameter

$$\xi \equiv \frac{L}{nr^2}, \tag{2}$$

where n is the hydrogen number density and r is the distance from the MBH (note the use of the bolometric luminosity in the definition of ξ). In the temperature range 2×10^4–10^7 K, to a good accuracy

$$T_{\rm eq}(\xi) \approx 2 \times 10^2 \xi \,{\rm K}, \tag{3}$$

while for $\xi \ll 100$ and $\xi \gg 5 \times 10^4$, $T_{\rm eq} \approx 10^4$ K and 2×10^7 K, respectively. $T_{\rm eq}$ is the temperature at which heating through Compton scattering and photoionization balances Compton cooling and cooling due to continuum and line emission, on the assumption that the plasma is in ionization equilibrium, appropriate for the problem under consideration. In Fig. 1 we plot lines of constant $T_{\rm eq}$ on the (r, $nL_{\rm Edd}/L$) plane for $M_{\rm BH} = 10^8 M_\odot$ and $M_{\rm BH} = 10^9 M_\odot$

[note that the full expression of $T_{\rm eq}(\xi)$ is used for this purpose].

Suppose now that the gravitational potential is due to the central MBH alone. Then the condition

$$\frac{5}{2}kT_{\rm eq}(\xi) - \frac{GM_{\rm BH}\mu m_{\rm p}}{r} > 0 \qquad (4)$$

(here $\mu = 0.61$ is the mean molecular weight) defines a situation where gas of density n, located at r, will be heated to $T_{\rm eq}$ by the central radiation and blown out of the MBH potential [1]. For given $M_{\rm BH}$, $L/L_{\rm Edd}$ and r, gas with density below a certain critical value, as implicitly given by equation (4), cannot accrete onto the MBH, which corresponds to the dashed areas in Fig. 1.

We now specify the general conditions above to Bondi accretion. Note that we are not assuming Bondi accretion onto the central MBH, since the infalling material is expected to possess non-negligible angular momentum and form an accretion disk or a more complicated central flow near the MBH[2]. We thus regard the Bondi relations as an indication of the flow rates into the central regions as a source of mass for the central flows.

The Bondi flow is transonic inside the radius

$$R_{\rm B} = \frac{GM_{\rm BH}\mu m_{\rm p}}{2\gamma kT} = 16\,{\rm pc}\frac{1}{\gamma}\frac{M_{\rm BH}}{10^8 M_\odot}\left(\frac{T}{10^6\,{\rm K}}\right)^{-1}, \qquad (5)$$

where T is the temperature at $R_{\rm B}$ and the sound speed $c_{\rm s} = \sqrt{\gamma kT/\mu m_{\rm p}}$. We shall assume $\gamma = 1$ (isothermal flow) for estimations below, the results depending very weakly on γ. Comparison of equation (4) with equation (5) shows that Bondi accretion of gas at temperature T can be disrupted if the central luminosity L is sufficiently high that $T_{\rm eq}(R_{\rm B}) \gtrsim T$, or equivalently $L > L_{\rm crit}$, where

$$L_{\rm crit}(T) = \xi(T)R_{\rm B}^2(T)n(R_{\rm B}), \qquad (6)$$

and $\xi(T)$ is the ionization parameter corresponding to $T_{\rm eq} = T$. *If $L > L_{\rm crit}$, the gas in the vicinity of $R_{\rm B}$ will experience net radiative heating.* On the other hand, the central luminosity is determined by the pre-existing conditions at $R_{\rm B}$ (so far as $L < L_{\rm Edd}$):

$$L = \epsilon c^2 \times 4\pi R_{\rm B}^2(T)c_{\rm s}(T) \times \mu m_{\rm p} n_{\rm t}(R_{\rm B}), \qquad (7)$$

where $n_{\rm t} \approx 2.3n$ is the total particle number density.

Fig. 2 (upper panel) shows the ratio $L/L_{\rm crit}$ as a function of gas temperature for three values of the accretion efficiency, $\epsilon = 0.01$, 0.05 and 0.1. The two higher values would correspond to accretion via a standard thin disk (Shakura & Sunyaev 1973). The presented curves have been obtained from equations (6) and (7) using the full expression

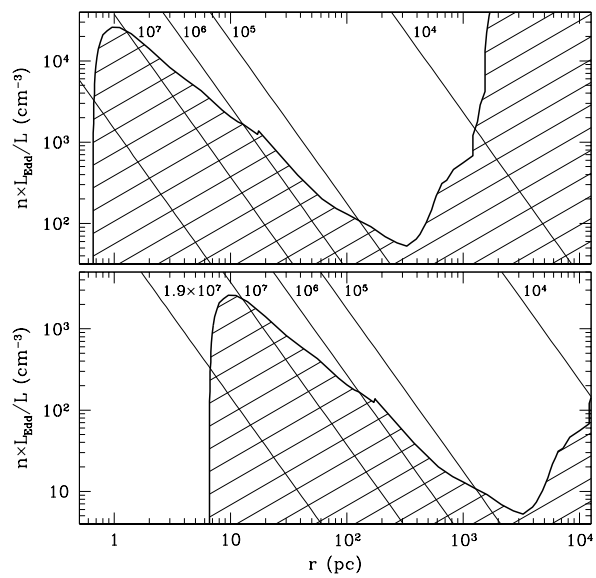

Figure 1. Energy-based gas escape condition near a black hole of mass $M_{\rm BH}$ in the (r, n) plane, under the assumption that the gas is in ionization equilibrium. Slanted lines correspond to constant values of the ionization parameter as given by equation (3) for different equilibrium gas temperature $T_{\rm eq}$ (labels along the lines). $T_{\rm eq}$ is shown up to the Compton temperature (1.9×10^7 K) characterizing the average quasar. The dashed area below the solid curve given in equation (4) corresponds to gas configurations energetically unbound. In the upper and lower panel $M_{\rm BH} = 10^8 M_\odot$ and $M_{\rm BH} = 10^9 M_\odot$, respectively.

of $T_{\rm eq}(\xi)$, and can be approximated in a limited temperature range by the expression

$$\frac{L}{L_{\rm crit}} \approx 6\frac{\epsilon}{0.1}\left(\frac{T}{10^6\,{\rm K}}\right)^{-1/2}, \; 2\times10^4\,{\rm K} < T < 10^7\,{\rm K}, \qquad (8)$$

which follows from equation (3). Note that the ratio $L/L_{\rm crit}$ does not depend on $M_{\rm BH}$. The fact that $L > L_{\rm crit}$ over most of the plot in Fig. 2 suggests that stationary accretion at high rates is impossible, unless the gas supplied into the Bondi sphere from outside is hotter than the Compton temperature of the average quasar SED, i.e. $T > T_{\rm C} \approx 2\times10^7$ K. If $T < T_{\rm C}$, the inflowing gas near $R_{\rm B}$ will be heated and driven out by the quasar radiation, and the MBH luminosity will be reduced for the time required for significant amounts of gas to cool and accumulate again in the central regions, i.e. the result will be relaxation oscillations.

However, such a dramatic heating effect as described above will only occur if the characteristic flow time at $R_{\rm B}$,

$$t_{\rm dyn} \equiv \frac{R_{\rm B}}{(2GM_{\rm BH}/R_{\rm B})^{1/2}} \approx 7\times10^4\,{\rm yr}\frac{M_{\rm BH}}{10^8 M_\odot}\left(\frac{T}{10^6\,{\rm K}}\right)^{-3/2}, \qquad (9)$$

is longer than the heating time scale

$$t_{\rm heat} \equiv \frac{n_{\rm t}(R_{\rm B})kT}{\Gamma(T,\xi)}. \qquad (10)$$

Here $\Gamma(T,\xi)$ is the plasma net heating (cooling) rate per unit volume, which in the case of the average quasar SED

[1] We note that in the case of the MBH emitting at near $L_{\rm Edd}$, the radiation pressure will effectively reduce the MBH gravitational potential, making possible an outflow in the directions not screened by the central accretion disk for lower values of ξ than implied by equation (4).

[2] In the case of quasars, it is believed that accretion occurs via a geometrically thin, optically thick disk, the presence of which naturally explains both the fact that most of the radiative output takes place at ultraviolet wavelengths and the inferred high radiative efficiency ($\epsilon \approx 0.1$) of accretion (e.g. Yu & Tremaine 2002). We briefly discuss the consequences of the presence of a central accretion disk at the end of this Section.

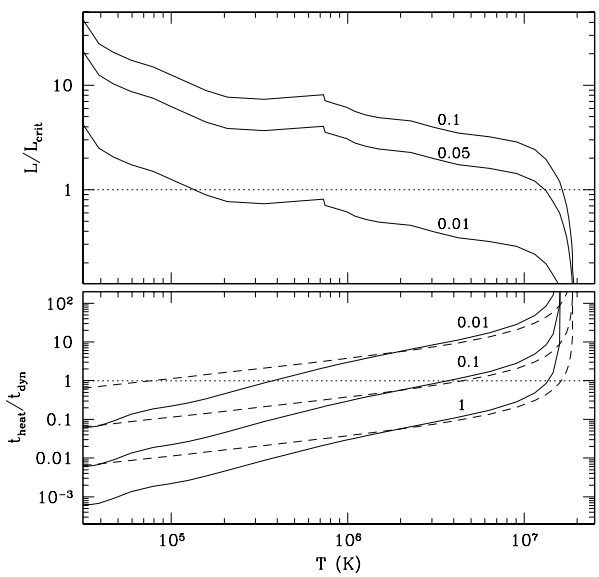

Figure 2. Top panel: the ratio $L/L_{\rm crit}$ as a function of T for Bondi accretion, as given by equations (6) and (7). The label above solid curves represents the adopted radiative efficiency. $L/L_{\rm crit} > 1$ implies that stationary accretion is impossible due to strong preheating. Bottom panel: ratio of the characteristic heating and flow times at the Bondi radius, as given by equations (9) and (10), as a function of the gas temperature T for $\epsilon = 0.1$ and different values of $L/L_{\rm Edd}$ (labels). Solid lines correspond to net heating, while dashed lines to Compton heating only. $t_{\rm heat}/t_{\rm dyn} > 1$ implies that radiative heating is inefficient.

can be estimated from formulae given in Appendix A3.3. Assuming $\epsilon = 0.1$, we find that for $L/L_{\rm crit}$ approximated by equation (8)

$$\Gamma \approx 3\times 10^{-23} n^2(R_{\rm B})\,{\rm erg\,s^{-1}\,cm^{-3}},$$

$$t_{\rm heat} \approx 2\times 10^3\,{\rm yr}\left(\frac{T}{10^6\,{\rm K}}\right)^{-1/2}\frac{M_{\rm BH}}{10^8 M_\odot}\left(\frac{L}{L_{\rm Edd}}\right)^{-1},$$

$$\frac{t_{\rm heat}}{t_{\rm dyn}} \approx 0.03\left(\frac{L}{L_{\rm Edd}}\right)^{-1}\frac{T}{10^6\,{\rm K}},\ 2\times 10^4\,{\rm K} < T < 10^7\,{\rm K}. \quad (11)$$

A more accurate computation leads to the curves shown in Fig. 2 (lower panel), giving the ratio $t_{\rm heat}/t_{\rm dyn}$ as a function of T for different values of $L/L_{\rm Edd}$. Also plotted is the ratio $t_{\rm C}/t_{\rm dyn}$ for the case of pure Compton heating/cooling. One can see that Compton preheating is important when $T \gtrsim 10^6$ K and $L \gtrsim 0.1 L_{\rm Edd}$. For $T < 10^6$ K, preheating due to photoionization is significant at even lower accretion rates.

The above discussion suggests that if quasars are fed by warm ($T < 10^7$ K) interstellar gas from distances ∼10–100 pc, their emission is expected to be significantly variable on time scales $\sim t_{\rm dyn}$ ∼10^4–10^5 years. Only for gas temperatures approaching 10^7 K, is stationary accretion at sub-Eddington rates possible (see Fig. 2).

We note however that, if the final stages of accretion occur via a geometrically thin or slim disk, as expected for quasars (see Footnote 2), the above conclusion should change as regards the variability time scale. Indeed, the characteristic viscous time in a geometrically thin, optically thick accretion disk is given by (Shakura & Sunyaev 1973)

$$t_{\rm visc}(r) \sim 3\times 10^5\,{\rm yr}\left(\frac{\alpha}{0.1}\right)^{-1}\left(\frac{L}{L_{\rm Edd}}\right)^{-2}\left(\frac{M}{10^8 M_\odot}\right)^{-2.5} \times\left(\frac{r}{0.01\,{\rm pc}}\right)^{3.5}, \quad (12)$$

where α is the viscosity parameter. The above formula is valid in the innermost, radiation pressure dominated zone of the disk, where the main source of opacity is Thomson scattering. Such disks, characterized by a radially constant accretion rate, are unlikely to extend beyond 10^{-3}–10^{-2} pc because they would become self-gravitating (Toomre 1964; Kolykhalov & Sunyaev 1980; Goodman 2003). Since the quasar life time is expected to exceed 10^7 yr, the accretion disk must be constantly replenished with gas of small angular momentum (presumably from a Bondi-type flow).

In the case of quasars ($M_{\rm BH} \gtrsim 10^8 M_\odot$, $L \gtrsim 0.1 L_{\rm Edd}$), self-gravity is expected to truncate the disk already in the innermost zone, at the distance

$$R_{\rm sg} \approx 0.014\,{\rm pc}\left(\frac{\alpha}{0.1}\right)^{2/9}\left(\frac{L}{L_{\rm Edd}}\right)^{4/9}\left(\frac{M}{10^8 M_\odot}\right)^{7/9}, \quad (13)$$

and the disk is expected to be stable against the thermal-viscous instability (Burderi, King & Szuszkiewicz 1998). Comparison of equations (9) and (12) implies that the timescale on which accreting matter drifts from the outer boundary of the disk to the MBH, $t_{\rm visc}(R_{\rm sg})$, can exceed the characteristic dynamical time of the external Bondi-type flow, $t_{\rm dyn}(R_{\rm B})$. In such a case, variations in the gas inflow rate at $R_{\rm B}$ as a result of preheating will affect the MBH accretion rate with a time delay $\sim t_{\rm visc}$, leading to variations in the quasar luminosity also on time scales $\sim t_{\rm visc}$.

2.2 Heating of ISM in spheroids

The gravitational potential of the central MBH is overcome by the potential of the host spheroid at distances larger than the MBH radius of influence

$$R_{\rm BH} \simeq \frac{GM_{\rm BH}}{\sigma^2} \approx 10\,{\rm pc}\frac{M_{\rm BH}}{10^8 M_\odot}\left(\frac{\sigma}{200\,{\rm km\,s^{-1}}}\right)^{-2}, \quad (14)$$

where σ is the characteristic (virial) one-dimensional stellar velocity dispersion in the galaxy. Comparison of equation (14) with equation (5) implies that $R_{\rm B} < R_{\rm BH}$ when $T \gtrsim T_{\rm vir}$, where

$$T_{\rm vir} \simeq \frac{\mu m_{\rm p}\sigma^2}{k} = 3.0\times 10^6\,{\rm K}\left(\frac{\sigma}{200\ {\rm km\ s^{-1}}}\right)^2 \quad (15)$$

is the galaxy virial temperature. Therefore, our discussion of preheating in §2.1 pertains to situations where the accreting flow has a temperature comparable to or higher than the galaxy virial temperature.

Below we assess the conditions required for the central MBH to significantly heat the interstellar gas over a substantial volume of the galaxy, regardless of the type of accretion flow established in the central regions. In this Section we shall *assume* that the MBH has a mass as given by the observed $M_{\rm BH}$-σ relation for local ellipticals and bulges (Tremaine et al. 2002):

$$M_{\rm BH} = 1.5\times10^8 M_\odot \left(\frac{\sigma}{200\ {\rm km\ s^{-1}}}\right)^4. \quad (16)$$

Note that this assumption will be dropped in §3, where we attempt to *predict* the $M_{\rm BH}$-σ relation.

From equations (15) and (16) we can find the critical density $n_{\rm crit}$, defined by

$$T_{\rm eq}(L/n_{\rm crit}r^2) = T_{\rm vir}, \quad (17)$$

as a function of distance r from the galaxy center. Gas with $n < n_{\rm crit}$ will be heated above $T_{\rm vir}$ and expelled from the galaxy, whereas gas cooling will dominate over Compton and photoionization heating if $n > n_{\rm crit}$. We show in Fig. 3 the resulting heating diagrams on the (r, n) plane for two galaxies, with $\sigma = 180$ and $320\,{\rm km\,s^{-1}}$, corresponding to $M_{\rm BH} = 10^8$ and $10^9 M_\odot$, respectively. Also shown in Fig. 3 is the $n(r)$ line at which the cooling time $t_{\rm cool,0}$ of gas at $T_{\rm vir}$ in the absence of radiative heating equals the characteristic dynamical time, $t_{\rm dyn} \equiv r/\sigma$. Gas with density above this line will cool down before reaching the galactic nucleus if there are no heating mechanisms other than gravitational compression. Comparison of the $T_{\rm eq} = T_{\rm vir}$ line with the $t_{\rm cool,0} = t_{\rm dyn}$ one implies that if the gas within a few kpc of the MBH is sufficiently tenuous to sustain a subsonic cooling flow (so that $t_{\rm cool,0} > t_{\rm dyn}$ and $T \approx T_{\rm vir}$), the central quasar emitting $L \gtrsim 0.1 L_{\rm Edd}$ will be able to heat the gas above $T_{\rm vir}$.

In practice, provided that $T_{\rm eq} > T_{\rm vir}$, significant heating will take place only out to a certain distance that depends on the luminosity and duration of the quasar outburst. Since the MBH releases via accretion a finite total amount of energy, $\epsilon M_{\rm BH} c^2$, there is a characteristic limiting distance given by:

$$\begin{aligned} R_{\rm C} &= \left(\frac{\sigma_{\rm T}\epsilon M_{\rm BH}}{3\pi m_{\rm e}}\right)^{1/2} = 400\,{\rm pc}\left(\frac{\epsilon}{0.1}\right)^{1/2}\left(\frac{M_{\rm BH}}{10^8 M_\odot}\right)^{1/2} \\ &= 500\,{\rm pc}\left(\frac{\epsilon}{0.1}\right)^{1/2}\left(\frac{\sigma}{200\ {\rm km\ s^{-1}}}\right)^2. \end{aligned} \quad (18)$$

Inside this radius, each electron–proton pair will have received at least $3kT_{\rm C} \approx 6\,{\rm keV}$ of energy through Compton scattering of hard X-rays from the MBH when it has accreted mass $M_{\rm BH}$. $R_{\rm C}$ is defined assuming that the only heating mechanism is Compton scattering, and thus pertains to the limit of low density gas, fully photoionized by the radiation from the MBH.

More relevant for the problem at hand is the distance out to which low density gas will be Compton heated to $T \geq T_{\rm vir}$:

$$R_1 = R_{\rm C}\left(\frac{T_{\rm C}}{T_{\rm vir}}\right)^{1/2} = 1,300\,{\rm pc}\left(\frac{\epsilon}{0.1}\right)^{1/2}\frac{\sigma}{200\ {\rm km\ s^{-1}}}. \quad (19)$$

Yet another characteristic radius is the one within which gas of critical density $n_{\rm crit}$ will be heated to $T \geq T_{\rm vir}$ by photoinization and Compton scattering:

$$R_2 = R_1\left[\frac{\Gamma(n_{\rm crit})}{\Gamma_{\rm C}}\right]^{1/2}, \quad (20)$$

where $\Gamma_{\rm C}$ and Γ are the Compton and total heating rates, respectively. Depending on the gas density ($0 < n < n_{\rm crit}$), the outer boundary of the "blowout region" will be located somewhere between R_1 and R_2. The size of the heating zone may be compared (see Fig. 3) with the galaxy effective (half-light) radius $R_{\rm e}$. We estimate from the results of Faber et al. (1997) and Bernardi et al. (2003) that for early-type galaxies

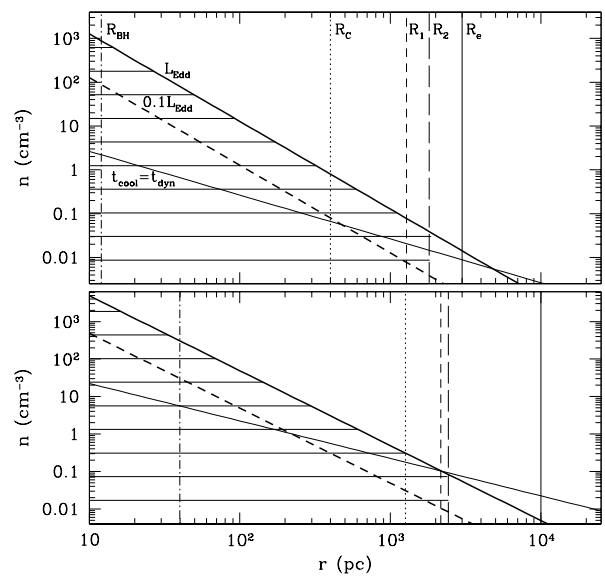

Figure 3. The (r, n) plane for a galaxy with $\sigma = 180\,{\rm km\,s^{-1}}$ ($T_{\rm vir} = 2.4\times10^6$ K, $M_{\rm BH} = 10^8 M_\odot$, upper panel), and with $\sigma = 320\,{\rm km\,s^{-1}}$ ($T_{\rm vir} = 7.7\times10^6$ K, $M_{\rm BH} = 10^9 M_\odot$, lower panel). In the dashed area gas can be heated above $T_{\rm vir}$ by radiation from the central MBH emitting at the Eddington luminosity. The upper boundary of this area scales linearly with luminosity (as shown by the dashed line corresponding to $L = 0.1 L_{\rm Edd}$). From left to right vertical lines correspond to $R_{\rm BH}$ [equation (14)], $R_{\rm C}$ [equation (18)], R_1 [equation (19)], R_2 [equation (20)], and $R_{\rm e}$ [equation (21)]. The thin slanted line bounds from the above the zone where the intrinsic cooling time of gas at $T_{\rm vir}$ is longer than the dynamical time. See text for further explanation.

$$R_{\rm e} \sim 4,000\,{\rm pc}\left(\frac{\sigma}{200\ {\rm km\ s^{-1}}}\right)^2, \quad (21)$$

and note that in reality the correlation between $R_{\rm e}$ and σ is fairly loose.

The different characteristic distances defined above are shown as a function of $M_{\rm BH}$ in Fig. 4. One can see that the radiative output of a black hole of mass $< 10^7 M_\odot$ can unbind the interstellar gas out to several $R_{\rm e}$ in relatively low luminosity elliptical galaxies. In the case of more massive black holes/galaxies with $M_{\rm BH} \sim 10^8$–$10^9 M_\odot$, the heating will be localized to the innermost 0.3–0.5$R_{\rm e}$; the gas further out can be heated only indirectly, presumably through shock waves propagating from the radiatively heated central regions (see CO01). Remarkably, $R_2 \approx 2$–$4\,{\rm kpc}$, almost independently of $M_{\rm BH}$. This results from a combination of two opposite trends: the lighter the MBH is, the less total energy it emits, and the lower $T_{\rm vir}$ is, the more important becomes the role of photoionization heating compared to Compton heating for gas with $n \lesssim n_{\rm crit}$. We point out that radiation characterized by the average quasar SED could not unbind the gas in galaxies with $\sigma > 500\,{\rm km\,s^{-1}}$

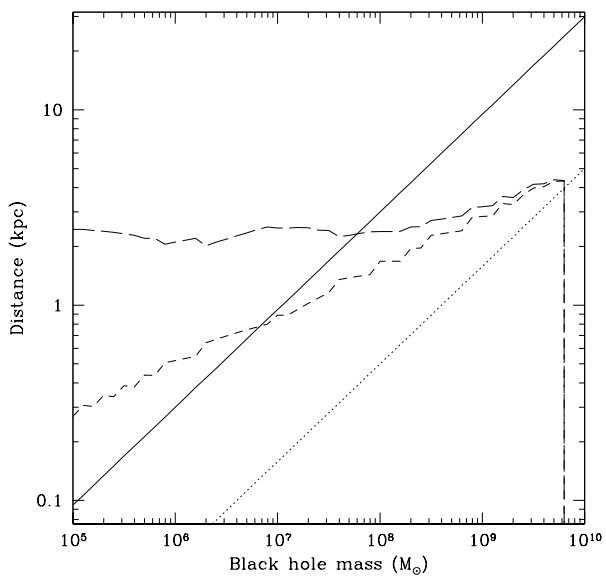

Figure 4. Different characteristic heating radii, $R_{\rm C}$ (dotted line), R_1 (short-dashed line), and R_2 (long-dashed line), as a function of $M_{\rm BH}$, compared with the general trend for the effective radius of elliptical galaxies (solid line).

($M_{\rm BH} > 6\times10^9 M_\odot$) if such giant galaxies existed, because then $T_{\rm vir} > T_{\rm C} \approx 2\times10^7$ K. On the contrary, the gas in the central regions of such galaxies would be *Compton cooled* by the radiation from the central quasar. Presumably it is a coincidence that the upper limit to the velocity dispersion for real elliptical galaxies is close to the Compton temperature found for the radiation from typical massive quasars.

We finally note that in the case of a quasar outburst with given L and duration t, during which a relatively small amount of mass $\Delta M_{\rm BH} \ll M_{\rm BH}$ is accreted, the radiative heating front will propagate out to

$$\tilde{R}_{1,2}(L,t) = R_{1,2}\left(\frac{L}{L_{\rm Edd}}\right)^{1/2}\left(\frac{t}{2\times10^7\,{\rm yr}}\right)^{1/2}\left(\frac{\epsilon}{0.1}\right)^{-1/2} \quad (22)$$

in time t, where $R_{1,2}$ are given by equations (19), (20). It is worth noting that in the case of Eddington-limited accretion, the characteristic heating time at $R_{1,2}$ is $2\times10^7(0.1/\epsilon)$ yr, or approximately half the Salpeter time scale (time required for the black hole mass to double).

3 THE PROPOSED ORIGIN OF THE $M_{\rm BH}$–σ RELATION

We now address the central issue of this work, namely the possibility that radiative feedback played the key role in establishing the observed $M_{\rm BH}$–σ relation.

Below we elaborate on the following general idea. Before the MBH grows to a certain *critical mass*, $M_{\rm BH,crit}$, its radiation will be unable to efficiently heat the ambient gas, and accretion onto the MBH will proceed at a high rate. Once the MBH has grown to $M_{\rm BH,crit}$, its radiation will heat and expel a substantial amount of gas from the central regions of the galaxy[3]. Feeding of the MBH will then become self-regulated on the cooling time scale of the low density gas. Subsequent quasar activity will be characterized by a very small duty cycle ($\sim$0.001), as predicted by hydrodynamical simulations (CO97, 01) and suggested by observations (Haiman et al. 2004; Heckman et al. 2004). MBH growth will be essentially terminated.

Suppose that the galaxy density distribution is that of a singular isothermal sphere, with the gas density following the total density profile:

$$\rho_{\rm gas}(r) = \frac{M_{\rm gas}}{M}\frac{\sigma^2}{2\pi G r^2}. \quad (23)$$

Here $M_{\rm gas}$ and M are the gas mass and and total mass within the region affected by radiative heating. The size of the latter is uncertain but is less than a few kpc (see §2.2), so that M is expected to be dominated by stars ($M_* \lesssim M$) rather than by dark matter.

Radiation from the central MBH can heat the ambient gas up to the temperature

$$T_{\rm eq} \approx 6.5\times10^3\,{\rm K}\frac{L}{L_{\rm Edd}}\left(\frac{M_{\rm gas}}{M}\right)^{-1}\frac{M_{\rm BH}}{10^8 M_\odot}\left(\frac{200\,{\rm km\ s^{-1}}}{\sigma}\right)^2. \quad (24)$$

This approximate relation is valid in the range 2×10^4–10^7 K and follows from equations (3) and (23). Remarkably, $T_{\rm eq}$ does not depend on distance for the adopted r^{-2} density distribution. We then associate the transition from rapid MBH growth to slow, feedback limited MBH growth with meeting the critical condition

$$T_{\rm eq} = \eta_{\rm esc} T_{\rm vir}, \quad (25)$$

where $\eta_{\rm esc} \gtrsim 1$ and $T_{\rm vir}$ is given by equation (15). Once heated to $T_{\rm eq} = \eta_{\rm esc} T_{\rm vir}$, the gas will stop feeding the MBH. We readily find that the condition (25) will be met for

$$M_{\rm BH,crit} = 4.6\times10^{10} M_\odot \eta_{\rm esc}\left(\frac{\sigma}{200\,{\rm km\ s^{-1}}}\right)^4\frac{L_{\rm Edd}}{L}\frac{M_{\rm gas}}{M}. \quad (26)$$

Therefore, for fixed values of $\eta_{\rm esc}$, $L/L_{\rm Edd}$ and $M_{\rm gas}/M$ we expect $M_{\rm BH,crit} \propto \sigma^4$, similar to the observed $M_{\rm BH}$–σ relation. According to our proposed scenario, once the MBH has reached the critical mass, its accretion growth will be effectively terminated so that at the present epoch $M_{\rm BH}$ is expected to be only slightly larger than $M_{\rm BH,crit}$.

Equally important information is contained in the normalization of the $M_{\rm BH}$–σ relation. In fact, by comparing equation (26) with equation (16) we find that the observed relationship will be established if

$$\frac{M_{\rm gas}}{M_*} = 3\times10^{-3}\eta_{\rm esc}^{-1}\frac{L}{L_{\rm Edd}}\frac{M}{M_*}. \quad (27)$$

To satisfy the observed $M_{\rm BH}$–σ relation, the gas-to-stars ratio is thus required to be relatively low and approximately constant for spheroids with different masses at the epoch when the MBH reaches its critical mass, although the observational uncertainty in the $M_{\rm BH}$–σ relation leaves some room for a weak dependence of $M_{\rm gas}/M_*$ on σ. As for the

[3] Quite obviously, this effect will cooperate with the energy input from stellar winds and SNII explosions in the forming galaxies, however here we show that in principle the radiative feedback from the MBH only is already sufficient to do the work.

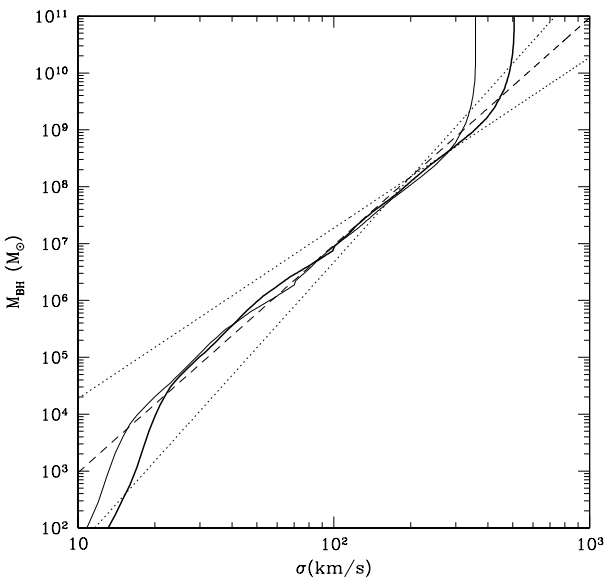

Figure 5. Thick solid line shows the predicted $M_{\rm BH}$–σ relation resulting from the requirement that heating of the interstellar gas by radiation from the central MBH at the Eddington limit be below the level required to drive the gas from the galaxy ($T_{\rm eq} \leq T_{\rm vir}$). This upper bound on $M_{\rm BH}$ is based on assuming a constant gas fraction of $M_{\rm gas}/M = 0.003$ and $\eta_{\rm esc} = 1$. The thin solid line corresponds to $M_{\rm gas}/M = 0.0015$ and $\eta_{\rm esc} = 2$. The dashed line is the observed $M_{\rm BH} \propto \sigma^4$ relation in the range $M_{\rm BH} = 10^6$–a few $10^9 M_\odot$, extrapolated to lower and higher $M_{\rm BH}$ values from equation (16). The dotted lines are $M_{\rm BH} \propto \sigma^3$ and $M_{\rm BH} \propto \sigma^5$ laws.

Eddington ratio, it is reasonable to expect $L/L_{\rm Edd}$ ~0.1–1 based on hydrodynamical simulations (CO01) and observations of quasars (see e.g. Haiman et al. 2004 and references therein).

We note that the above calculation was based on a specific (r^{-2}) gas density profile for which $\xi = L/nr^2 = const.$ This allowed us to avoid specifying the size of the radiative heating zone. Being a reasonable assumption for the outer regions of the galaxy, the r^{-2} profile is however expected to flatten in the central ~$0.1R_{\rm e}$ region (see, e.g., CO01), so that ξ will be increasing toward the MBH. Since it can be sufficient to overheat the cooling gas in this central zone to produce dramatic effects on the subsequent co-evolution of the galaxy and its central MBH, our scenario certainly allows the critical $M_{\rm gas}/M_*$ ratio (defined say within $R_{\rm e}$) to be several times larger than required by equation (27).

We note that the approximately linear $T_{\rm eq}(\xi)$ dependence [see equation (3)] was crucial to the above argument leading to the $M_{\rm BH,crit} \propto \sigma^4$ result. However, the $T_{\rm eq}(\xi)$ function becomes strongly nonlinear outside the range $2 \times 10^4\,{\rm K} < T_{\rm eq} < 10^7\,{\rm K}$, and a more general result can be obtained if we consider the exact curve $T_{\rm eq}(\xi)$ from SOS. In Fig. 5 we show the predicted correlation between $M_{\rm BH,crit}$ and σ for $\eta_{\rm esc} = 1$, $L/L_{\rm Edd} = 1$ and $M_{\rm gas}/M = 3\times10^{-3}$, and compare it with the observed relationship. We see that the $M_{\rm BH} \propto \sigma^4$ behavior is expected to break down for $M_{\rm BH} < 10^4 M_\odot$ and also for $M_{\rm BH} \gtrsim$ a few $10^9 M_\odot$. In the same figure we demonstrate the effect of the escape parameter $\eta_{\rm esc}$. For $\eta_{\rm esc} = 2$ and the gas fraction decreased two-fold, the $M_{\rm BH}$–σ relation is unchanged except that the high-mass cutoff occurs at a lower mass. Specifically $M_{\rm BH,cut} \approx 3 \times 10^9 M_\odot \eta_{\rm esc}^{-2}$.

It is perhaps interesting that the range of masses shown in Fig. 5 for which $M_{\rm BH} \propto \sigma^4$ is obtained from considerations of atomic physics (and the observed AGN spectra) corresponds closely with the range of masses for which this power law provides a good fit to the observations. Exploring the $M_{\rm BH}$–σ relation observationally near $10^9 M_\odot$ would be a sensitive test of the importance of radiative feedback. We note that other scenarios discussed in the literature also predict deviations from the power law trend for the most massive MBHs (e.g. Menci et al. 2003).

4 A SIMPLE, PHYSICALLY BASED TOY-MODEL

In this Section we address in a more quantitative way the MBH–galaxy co-evolution. We adopt a physically-motivated one-zone model described in detail in Appendix A, focusing in particular on the co-evolution of the galaxy gas budget and stellar mass, a key ingredient of the proposed scenario (see Sect. 3). Several aspects of this model have been already described in Ciotti, Ostriker & Sazonov (2004) and Ostriker & Ciotti (2004).

In particular, source terms for the galaxy gas mass (equation [A1]) are due to cosmological infall (equation [A2]) and to stellar mass return from the evolving stellar population (equation [A4]), while gas is subtracted from the total budget by star formation (equation [A3]), gaseous MBH accretion (equation [A6]), and (possible) galactic winds when the thermal energy of the ISM is high enough to escape from the galaxy potential well (equation [A7]). Energy input on the galactic gas is due to thermalization of SNII and SNIa explosions, to thermalization of red giants winds due to the galaxy stellar velocity dispersion (Sects. A3.1 and A3.2), and to the radiative feedback from the accreting MBH (Sect. A3.3). In case of galactic winds, we also consider adiabatic cooling of the expanding gas (Sect. A3.4). Stars are formed by gas cooling, while *two* different mechanisms are considered for the MBH growth, namely gaseous accretion and coalescence of stellar remnants of massive stars (equation A5). The galaxy potential well is determined only by the dark matter potential well, which is assumed to be unevolving with cosmic time. In other words, here we are not considering merging between galaxies; finally, we note that in the present toy-model the possibility to add a simple recipe for chemical evolution is straightforward, so that one could also test the model against scaling laws such as the Mg_2–σ relation.

We remark here that this kind of approach is not new (e.g. Granato et al. 2004; Menci et al. 2003). However, our scenario presents a few but important differences with respect to the other cases. For example, in their modelization of the AGN feedback Granato et al. (2004) (see also Murray et al. 2004) assumed that the main role is played by radiation pressure through scattering and absorption by dust and scattering in resonance lines, while the energy release from the AGN to the ISM is due to thermalization

of the kinetic energy of the outflow. In our case, instead, the feedback is due to *radiative* heating. Note that energy absorption is typically more efficient in driving winds than momentum absorption.

Obviously, the results of such an approach should not be "overinterpreted": as common in all similar approaches, the parameter space of the present model is huge (even though several input parameters are nicely constrained by theory and/or observations), thus the results of such kind of simulations should be interpreted more as indications of possible evolutionary histories than exact predictions. In particular, the *toy-model cannot directly test the ability of radiative feedback to produce the right final MBH mass*, in fact, this can be done only using numerical hydrodynamical simulations. This is not surprising, because the toy-model, by construction, is a *one zone* model, and we already know that feedback mechanisms are strongly scale-dependent, in the sense that central galaxy regions react in a substantially different way with respect to the whole system (CO97, CO01, Sect. 2.2).

As a consequence, one of the key input parameters in our scheme is the adopted "quasar duty cycle" $f_{\rm Edd}$ [equation (A6)], which essentially introduces a limit, $f_{\rm Edd}L_{\rm Edd}$, on the instantaneous central quasar luminosity that is smaller than the Eddington luminosity. In the following, we present the results for two different assumptions about $f_{\rm Edd}$. In the first (Sect. 4.1), we distinguish two evolutionary phases: a first phase (the "cold phase", in which $\tau_{cool}/\tau_{dyn} < 1$) that would be identified observationally with the Lyman Break Galaxies, and a later phase (the "hot phase", in which $\tau_{cool}/\tau_{dyn} > 1$) that would be identified with normal, local ellipticals which contain little gas, have low rates of star formation and have a duty cycle (fraction of time during which they appear as luminous AGNs) of roughly 0.1%. Thus, in equation (A6) the duty cycle factor is known empirically to be $f_{\rm Edd} \simeq 0.01$ in the cold phase (where roughly a few per cent of Lyman Break Galaxies show central AGNs, Steidel et al. 2002; Lehmer et al. 2004), while $f_{\rm Edd} \simeq 0.001$ in the hot phase. It is important to note that the last value is suggested by both numerical simulations (CO01) and observations (Haiman et al. 2004).

A different model is also explored (Sect. 4.2), in which $f_{\rm Edd}$ is kept fixed to 1 over all the simulation. This case will adequately demonstrate the effects of radiative feedback on the toy-model evolution.

4.1 Models with reduced $f_{\rm Edd}$

With the above remarks in mind, here we present a few representative simulations primarily aimed at investigating whether there exists a specific evolutionary phase characterized by a gas-to-star mass ratio of the order of the factor in equation (27), required to obtain the right $M_{\rm BH}$–σ relation. The time evolution of the quantities shown in Figs. 6–8 refers to a galaxy reference model characterized by $R_{\rm e} = 4\,{\rm kpc}$ and a halo (constant) circular velocity of $400\,{\rm km\,s^{-1}}$; the total mass of the gas infall is $10^{11}M_\odot$, and the characteristic infall time is 2 Gyr. Other relevant simulations parameters are $\alpha_* = 0.3$ in equation (A3), $\beta_{BH,*} = 1.5\times10^{-4}$ in equation (A5), $\epsilon = 0.1$ in equation (A17), $\eta_{SN} = 0.5$ in equation (A27), and finally $\eta_{\rm esc} = 2$ in equation (A7). The initial black hole mass is assumed to be $10M_\odot$, and the duty-cycle is fixed according to the prescription of the "cold/hot" phases described above.

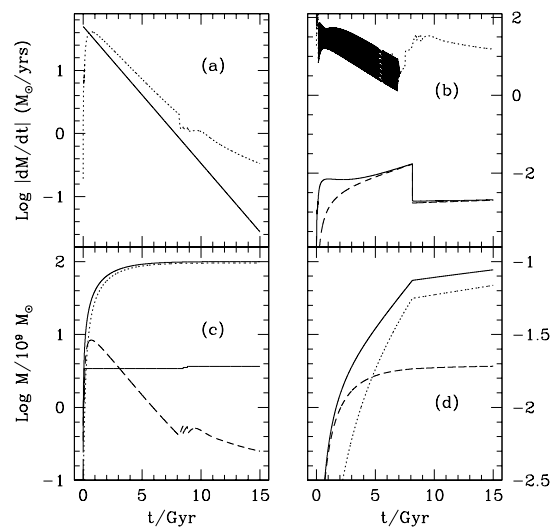

Figure 6. Reference model. Panel *a*: mass infall rate (solid line) and stellar mass formation rate (dotted line). Panel *b*: total (gaseous plus stellar remnants) MBH accretion rate (solid line), Bondi accretion rate (dotted line), Eddington accretion rate (reduced by the duty-cycle factor $f_{\rm Edd}$, dashed line). Panel *c*: total infall mass (solid line), total stellar galaxy mass (dotted line), total galaxy gas mass (short-dashed line); the nearly horizontal line is the escaped gas mass. Panel *d*: total MBH mass (solid line), total mass gaseously accreted (dotted line), MBH mass originated from stellar remnants (dashed line).

While a complete description of the toy-model behavior for different choices of the input parameters is outside the scope of this paper, here we remark that after an initial "cold" phase dominated by gas infall, as soon as the gas density becomes sufficiently low (Fig. 6c), and correspondingly the cooling time becomes longer than the dynamical time (Fig. 7d), the gas heating dominates, and the galaxy switches to a "hot" solution (Fig. 8). The gas mass/stellar mass ratio at that moment (~ 0.003, Fig. 7c) is very near with the value inferred in Section 3 from the argument leading to the right $M_{\rm BH}$–σ relation. Note also how the gas content of the present day "galaxy" is in nice agreement with observations. It proves that if $f_{\rm Edd}$ is sufficiently small (as in the present case), the accretion is Eddington (rather than Bondi) limited (equation [A6]) throughout the MBH–galaxy co-evolution, and then our model increases the MBH mass in the prescribed way *independently* of the specific feedback mechanism. The obtained final black hole mass is in nice agreement with the Magorrian relation (dotted line, Fig. 7b), but the significance of this result should not be overestimated since in reality the Magorrian relation is set (in our scenario) by the MBH feedback.

An interesting experiment is obtained by reducing the circular halo velocity and the infall mass in the reference model: in these cases galactic winds are favoured. In other words, small galaxies lose their gas content easily, in accor-

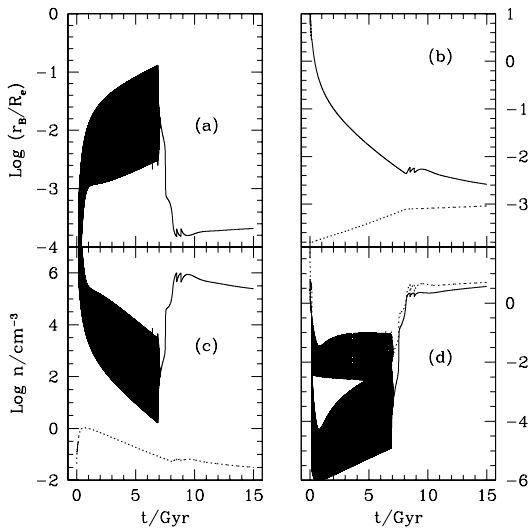

Figure 7. Reference model. Panel *a*: time evolution of the Bondi radius. Panel *b*: logarithm (base 10) of the ratio between gas mass to stellar mass (solid line) and of the ration between MBH mass to stellar mass ("Magorrian relation", dotted line). Panel *c*: gas density at the Bondi radius (solid line) and mean gas density (dotted line). Panel *d*: logarithm (base 10) of the cooling time (solid line) and heating time (dotted line) measured in terms of the dynamical tyme.

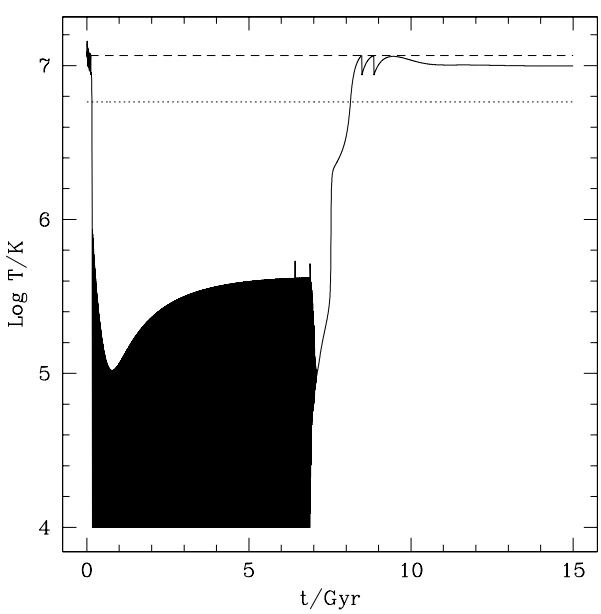

Figure 8. Time evolution of the model gas temperature (solid line). The model virial temperature is represented by the dotted line, while the dashed line represent the "escape" temperature (here assumed $2T_{\rm vir}$).

dance with the Mg_2–σ and the Faber–Jackson relations and with the hydrodynamical simulations of CO01. Remarkably, the transition to the hot phase of these models happens for $M_{\rm gas}/M_* \sim 0.01$, similarly to the behavior seen in the case of the more massive spheroid in the reference model. In other models we have verified the role of the AGN photoionization by artificially excluding the sources of stellar heating in the reference model: in this case the galaxy gas temperature (after the initial cold phase) remains sub-virial (i.e. below the horizontal dotted line in Fig. 8), without however cooling down to the imposed lower temperature limit of 10^4 K, as instead happens if we also exclude the MBH feedback. This sort of cooperation between AGN feedback and stellar energy injection, i.e., the fact that *substantial galactic winds in general are due to stellar heating, and are reinforced by the presence of the central AGN*, was already found in numerical simulations (CO01).

An important and apparently robust conclusion that can be drawn from these simulations is that stellar heating inevitably leads to a transition from cold to hot solution when the gas-to-star mass ratio drops to of order 1 per cent or somewhat less. Now, since a gas fraction of this order is required for the radiative feedback from the central MBH to limit its growth at the mass obeying the observed $M_{\rm BH}$–σ relation (see Sect. 3), it is tempting to suggest that the MBH reaches its critical mass, determined by radiative feedback, approximately at the epoch of transition from cold to hot galaxy phase.

We emphasize again that in the above models the radiative output from the MBH does not strongly influence the interstellar gas, since $f_{\rm Edd}$ is assumed to be low and thus the central luminosity is forced to be less than $f_{\rm Edd}L_{\rm Edd} \ll L_{\rm Edd}$ at any instant. In other words, these models allow persistent moderate AGN activity but forbid quasar-type outbursts.

4.2 A model illustrating radiative feedback

In order to illustrate the effects of MBH feedback in the context of the toy model, we now present a model in all similar to reference model (Sect. 4.1), but in which $f_{\rm Edd} = 1$ over all the evolution. In this model we also reduce the characteristic infall time from 2 Gyr to 0.2 Gyr, and we set $\beta_{BH,*} = 0$ in equation (A5), i.e., we are neglecting black hole growth due to accretion of stellar remnants.

Several differences are apparent with respect to the evolution of the reference model and its variants. In fact, the final black hole mass is now larger, the final amount of gas in the galaxy is significantly lower, and the galaxy is found in a permanent wind state (excluding the very short initial cold phase). Also, from Fig. 9b is apparent how the MBH grows by Bondi accretion instead of being Eddington limited (again excluding the initial phase). The main difference, however, is that now a very strong gas outflow is caused by the MBH feedback rather than by energy input from the evolving stellar population.

Most importantly, this model supports the argument presented in Section 3 in that quasar radiative heating terminates the MBH growth at a mass proportional to the gas fraction at the critical epoch, i.e. when the MBH feedback becomes important. The fact that in this particular simulation the final black hole mass turns out to be about 2 orders of magnitude higher than the "Magorrian" mass is

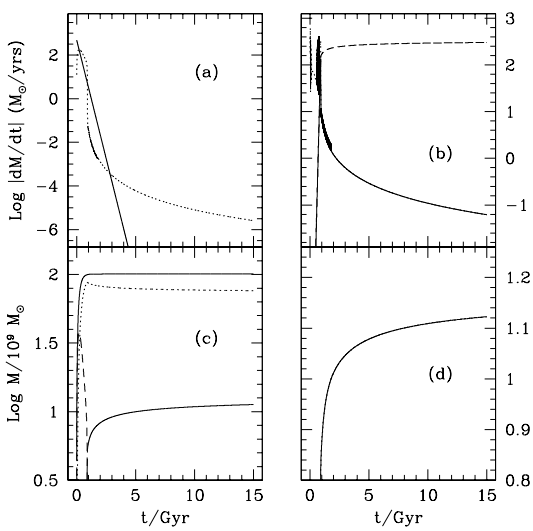

Figure 9. Model with $f_{\rm Edd} = 1$ and $\tau_{inf} = 0.2$ Gyr. See Caption of Fig. 6 for a description of the various curves. Note also how in the hot phase MBH accretion is Bondi dominated.

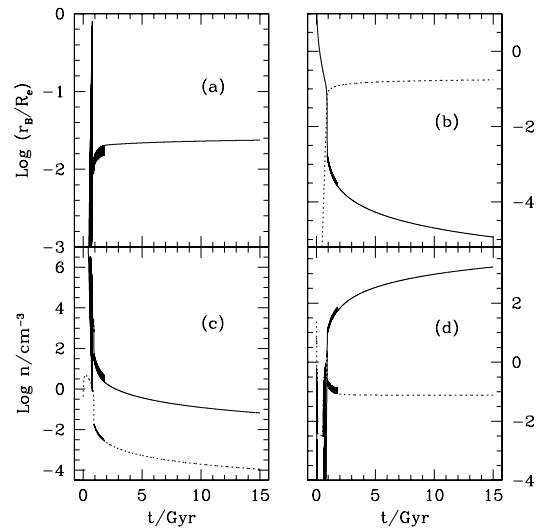

Figure 10. Same model as in Fig. 9. See Caption of Fig. 7 for a description of teh various curves.

due to the fact that the radiation from the central quasar overheats the gas when its mass fraction is ~ 10 per cent (see Fig. 10b), much higher than a fraction of 1 per cent. This happens in this model because the Eddington limited growth of the black hole allowed it to reach a very high mass while the galaxy gas content has not yet been reduced to low levels.

An obvious problem with the models described in Sections 4.1 and 4.2 is that the parametrization of the MBH accretion rate and luminosity in terms of the time averaged $f_{\rm Edd}$ factor is a very poor substitute for considering the real, time dependent problem. Nevertheless, we believe that the models assuming a small $f_{\rm Edd}$ and the model in which $f_{\rm Edd} = 1$ nicely complement each other and provide important clues to the real picture of MBH–galaxy co-evolution. Specifically, the first kind of models demonstrate that there is indeed a well defined phase in galactic evolution when the gas-to-stars mass ratio is of the order of 1 per cent – it corresponds to the transition from cold to hot solution. On the other hand, the $f_{\rm Edd} = 1$ model demonstrates how the MBH radiative feedback can be efficient if the central quasar switches on at a near Eddington luminosity. Taken together, these models suggest that a major quasar outburst occuring approximately at the beginning of the hot galaxy phase, when $M_{\rm gas}/M_* \sim 0.01$ or somewhat less, can lead to a significant degassing of the galaxy and termination of the MBH growth at the mass required by the $M_{\rm BH}$–σ relation.

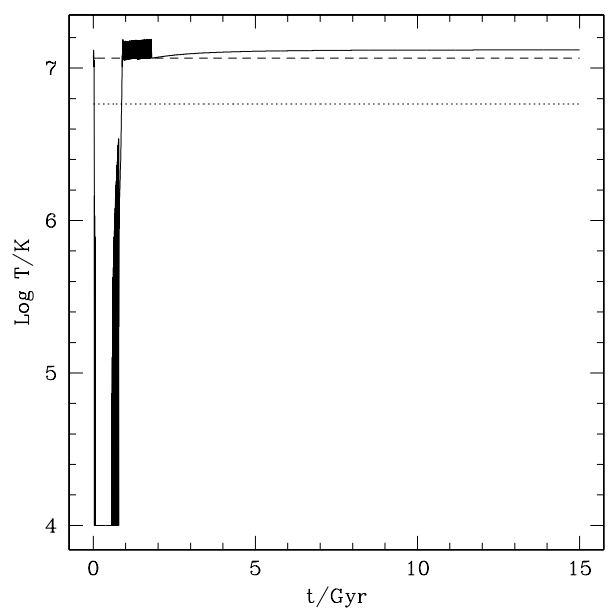

Figure 11. Temperature evolution of the model in Figs. 9 and 10. See Caption of Fig.8 for a description of the various curves. Note how the galaxy is found in a permanent wind phase after $\simeq 1$ Gyr.

5 DISCUSSION AND CONCLUSIONS

In this paper we explore the possible role of AGN radiative feedback in the co-evolution of MBHs at the center of spheroids and their stellar and gaseous components. The feedback is due to a combination of photoionization and Compton heating. In our calculations we adopt (from the work of SOS) a broad-band spectral energy distribution that corresponds closely with the radiative output of typical quasars.

We first investigate (Sect. 2.1), based on energetic considerations, whether the radiative output of the central MBH can significantly affect a Bondi-type accretion flow in the central 1–100 pc of a galaxy. In agreement with previous

studies, we find that if the accretion is radiatively efficient and proceeds at a subcritical rate, as expected of quasars, the mass inflow rate and the MBH luminosity are expected to oscillate on time scales $\sim 10^4$–10^5 yr as a result of gas preheating, unless the temperature of the supplied interstellar gas approaches the Compton temperature of the radiation field (2×10^7 K). We also note that if a central accretion disk extends beyond $\sim$0.001–0.01 pc from the MBH, then preheating of the external, hot flow may still lead to variations in the MBH accretion rate, but on longer time scales (up to millions of years), determined by the characteristic drift time in the disk.

Using similar energetic considerations, we then assess the effect of the MBH radiative feedback on the main volume of the host galaxy (Sect. 2.2). We demonstrate that the radiative output from a MBH growing by radiatively efficient accretion can unbind the ambient interstellar gas, provided it is tenuous enough, out to a maximum distance of a few kpc, which would typically amount to a significant fraction of the effective radius for giant ellipticals and to a few effective radii for smaller spheroids.

We then discuss (Sect. 3) a possible origin of the observed $M_{\rm BH}$–σ relation based on the hypothesis that the radiative output from the growing MBH will eventually heat the ambient interstellar gas above the virial temperature and expel most of it, limiting both future growth of the MBH and future star formation to low levels. We demonstrate that if the gas-to-stars mass ratio drops to $\lesssim$1 per cent in the central regions of spheroids at a certain stage of their evolution, then the radiative feedback from the central MBH switched on as a bright quasar will terminate its growth at the mass obeying the observed $M_{\rm BH}$–σ relation. Furthermore, we predict that the observed power law should break down for black hole masses below $10^4 M_\odot$ and above a few $10^9 M_\odot$. These considerations however leave open the question as to why the gas fraction should be of the above order when the MBH reaches the critical mass.

In order to obtain a better insight into the co-evolution of gas, stars and the central MBH over the Hubble time we explore a simple but physically based one-zone toy model (Sect. 4). A robust result obtained from the simulations is that when the gas mass fraction has been reduced by star formation to of order 1 per cent or somewhat less, a transition from cold to hot solution takes place, both in the case of massive protogalaxies that would evolve into the present day giant ellipticals and in the case of smaller spheroids. This transition occurs primarily as a result of gas heating due to the evolving galaxy stellar component in its various forms (stellar winds thermalization, SNII and SNIa explosions), while the AGN heating is also expected to contribute at some level.

The near coincidence of the gas fraction corresponding to the beginning of the hot galactic phase with that [equation (27)] required by our argument leading to the correct $M_{\rm BH}$–σ relation offers the possibility of the following evolutionary scenario. At the early stages of galaxy evolution when the protogalactic gas is dense and cold, active star formation is accompanied by the growth of a central black hole. The black hole however is not massive enough to produce a strong heating effect on the ambient, dense gas, even during episodes when it shines near at the Eddington limit. This cold phase would be identified observationally with the Lyman Break Galaxies and bright submillimeter galaxies, which are characterized by high star formation rate and moderate AGN activity. The cold phase ends when the gas-to-stars mass ratio has been reduced to $\sim$ 0.01, when the energy input from the evolving stellar population and possibly from the central MBH heat the gas to a sub-virial temperature. The MBH continues to grow actively during this transitional epoch (perhaps more actively than before) because there are still sufficient supplies of gas for accretion, and soon reaches the critical mass (obeying the $M_{\rm BH}$–σ relation), when the MBH radiative output causes a major gas outflow. This phase would be identified with the major quasar epoch. The subsequent evolution is passive and characterized by very low AGN activity and a duty cycle reduced by a factor of ten to 0.001, and this late phase would be identified with the present day elliptical galaxies.

This scenario is admittedly tentative and not the only possible one, and should be verified by observations and more detailed computations. In particular, it should be elucidated as to why the MBH does not grow to an excessive mass during the cold galactic phase, a key assumption implicitly made above. Possibly this does not happen, as also suggested in other works (e.g. Archibald et al. 2002), just because the stellar spheroid is formed too rapidly even compared to an Eddington limited growth of the MBH from an initial stellar mass up to 10^8–$10^9 M_\odot$, which takes $\lesssim$1 Gyr. Alternatively, early MBH growth may be characterized by some duty cycle determined by the poorly understood physics of gas supply and accretion on to protogalaxies.

A proper investigation of the importance of radiative heating on the MBH–galaxy co-evolution, based on high spatial hydrodynamical numerical simulations and adopting the specification of the input spectrum and atomic physics from this work, is now in progress (Ciotti & Ostriker, in preparation).

ACKNOWLEDGMENTS

REFERENCES

Alexander D.M. et al., 2003, AJ, 125, 383

Archibald E.N., Dunlop J.S., Jimenez R., Friaça. A.C.S., McLure R.J., Hughes D.H., 2002, MNRAS, 336, 353

Bernardi M., Sheth R.K., Annis J., Burles S., Eisensrein D.J. et al., 2003, AJ, 125, 1849

Binney J., Tabor G., 1995, MNRAS, 276, 663

Burderi L., King A., Szuszkiewicz E., 1998, ApJ, 509, 85

Burkert A., Silk J., 2001, ApJ, 554, L151

Cavaliere A., Vittorini V., 2002, ApJ, 570, 114

Churazov E., Sunyaev R., Forman W., Böhringer H., 2002, MNRAS, 332, 729

Ciotti L., D'Ercole A., Pellegrini S., Renzini A., 1991, ApJ, 376, 380 (CDPR)

Ciotti L., Ostriker J.P., 1997, ApJ, 487, L105 (CO97)

Ciotti L., Ostriker J.P., 2001, ApJ, 551, 131 (CO01)

Ciotti L., Ostriker J.P., Pellegrini S., 2004, Proceedings of the International Symposium "Plasmas in the laboratory and in the universe: new insights and new challenges", G. Bertin, D. Farina, R. Pozzoli eds., AIPCS, vol.703, p.367, 2004

Ciotti L., Ostriker J.P., Sazonov S. Yu., Proceedings of

the MPA/MPE/ESO/USM Conference "Growing Black Holes - Accretion in a cosmological context", ESO Astrophysics Symposia, A. Merloni, S. Nayakshin and R. Sunyaev eds., in press
Ciotti L., van Albada T., 2001, ApJ, 552, L13
Cowie L.L., Ostriker, J.P., Stark A.A., 1978, ApJ, 226, 1041
Faber S.M. et al., 1997, AJ, 114, 1771
Fabian A., 1999, MNRAS, 308, L39
Ferrarese L., Merritt D., 2000, ApJ, 539, L9
Goodman J., 2003, MNRAS, 339, 937
Granato G.L., Silva L., Monaco P., Panuzzo P., Salucci P., De Zotti G., Danese L., 2001, MNRAS, 324, 757
Granato G.L., De Zotti G., Silva L., Bressan A., Danese L., 2004, ApJ, 600, 580
Haiman Z., Ciotti L., Ostriker J.P., 2004, ApJ, 606, 763
Hamann F., Ferland G., 1999, ARA&A, 37, 487
Heckman T.M., Kauffmann G., Brinchmann, J., Charlot S., Tremonti C., White S.D.M., 2004, ApJ, 613, 109
Kallman T.R., 2002, XSTAR Manual, version 2.1 (Greenbelt, MD: NASA/GSFC)
King A., 2003, ApJ, 596, L27
Kolykhalov P.I., Sunyaev R.A., 1980, Sov. Astron. Lett., 6, 357
Krolik J.H., London R.A., 1983, ApJ, 267, 18
Lehmer B.D. et al., 2004, astro-ph/0409600
Magorrian J., Tremaine S., Richstone D., Bender R., Bower G., Dressler A. et al., 1998, AJ, 115, 2285
Mathews W.G., Bregman J.N., 1978, ApJ, 224, 308
Menci N., Cavaliere A., Fontana A., Giallongo E., Poli F., Vittorini V., 2003, ApJ, 587, L63
Murray N., Quataert E., Thompson T.A., astro-ph/0406070
O'Sullivan E., Forbes D.A., Ponman T.J., 2001, MNRAS, 328, 461
Ostriker J.P., Ciotti L., Phil.Trans. of Roy.Soc., part A, in press
Park M.-G., Ostriker J.P., 1999, ApJ, 527, 247
Renzini A. Ciotti L., D'Ercole A., Pellegrini S., 1993, ApJ, 419, 52
Sazonov S.Yu., Ostriker, J.P., Sunyaev R.A., 2004, MNRAS, 347, 144 (SOS)
Shakura N.I., Sunyaev R.A., 1973, A&A, 24, 337
Silk J., Rees M.J., 1998, A&A, 331, L1
Springel V., Di Matteo, T., Hernquist L., 2004, astro-ph/0409436
Steidel C.C. et al., 2002, ApJ, 576, 653
Toomre A., 1964, ApJ, 139, 1217
Tremaine S., Gebhardt K., Bender R., Bower G., Dressler A., Faber S.M. et al., 2002, ApJ, 574, 740
Wyithe J.S.B., Loeb A., 2003, ApJ, 595, 614
Yu Q., Tremaine S., 2002, ApJ, 335, 965

APPENDIX A: A TOY MODEL FOR THE MBH GROWTH

A1 The equations

The equations describing the evolution of the physical quantities considered in the present toy-model are

$$\dot{M}_{gas} = \dot{M}_{inf} - \dot{M}_* + \dot{M}_{rec} - \dot{M}_{BH} - \dot{M}_{esc}, \tag{A1}$$

$$\dot{M}_{inf} = \frac{M_{gal}}{\tau_{inf}} \exp\left(-\frac{t}{\tau_{inf}}\right), \tag{A2}$$

$$\dot{M}_* = \frac{\alpha_* M_{gas}}{\max(\tau_{dyn}, \tau_{cool})} - \dot{M}_{rec}, \tag{A3}$$

$$\dot{M}_{rec} = \int_0^t \dot{M}_*^+(t') W_*(t-t')\, dt', \tag{A4}$$

where $\dot{M}_*^+$ is the first term on the r.h.s. of equation (A3)

$$\dot{M}_{BH} = \dot{M}_{BH,acc} + \beta_{BH,*}\dot{M}_*^+, \tag{A5}$$

where

$$\dot{M}_{BH,acc} = \min(f_{\rm Edd}\dot{M}_{\rm Edd}, \dot{M}_{\rm B}), \tag{A6}$$

and finally

$$\dot{M}_{esc} = \begin{cases} \dfrac{M_{gas}}{\tau_{esc}}, & T \geq \eta_{\rm esc} T_{\rm vir}, \\ 0, & T < \eta_{\rm esc} T_{\rm vir}. \end{cases} \tag{A7}$$

A2 Input physics

A2.1 Gas equilibrium distribution

The code is started by assigning the dark-matter halo circular velocity v_c under the assumption of a (singular) isothermal distribution [see equation (23)], and the quantity τ_{dyn} entering equation (A3) is defined as

$$\tau_{dyn} \equiv \frac{2\pi R_{\rm e}}{v_c}, \tag{A8}$$

where $R_{\rm e}$ is a characteristic scale-length that could be identified with the effective radius or the half-mass radius of the gas and galaxy stellar distribution. For example, the radial trend of the gas density is obtained by *arbitrarily* imposing that all the gas mass is contained within $2R_{\rm e}$, and it is distributed as the dark matter halo:

$$\rho = \frac{\bar{\rho}_e}{3}\left(\frac{R_{\rm e}}{r}\right)^2. \tag{A9}$$

The assumption above should not taken too literally, in the sense that it is only a simple way to obtain a representative value of the mean gas density $\bar{\rho}_e$: different choices would lead to different values of $\bar{\rho}_e$ for an assigned total gas mass. In any case, as a consequence of our assumption, the *mean gas density* within $R_{\rm e}$ is given by

$$\bar{\rho}_e = \frac{3M_{gas}}{8\pi R_{\rm e}^3}. \tag{A10}$$

The (mass-weighted) equilibrium gas temperature $T_{\rm vir}$ could be obtained from the hydrostatic equilibrium and Jeans equations. However it is well known that a gas distribution as that in equation (A9) but untruncated (and so characterized by an infinite mass) would have the (constant) temperature

$$T_{\rm vir} = \frac{\mu m_p \sigma^2}{k} = \frac{\mu m_p v_c^2}{2k}, \tag{A11}$$

where we recall that for the singular isothermal sphere $\sigma^2 = v_c^2/2$, where σ is the (1-dimensional) halo velocity dispersion, and $\mu = 0.61$. For simplicity we use equation (A11) as an estimate of the equilibrium gas temperature associated with the density distribution in equation (A9).

A2.2 Gas cooling time

The *gas mean cooling time* within $R_{\rm e}$ is defined as $\tau_{cool} \equiv E/\dot{E}_C$, where

$$E = \frac{3k\bar{\rho}_e T}{2\mu m_p} \tag{A12}$$

is the gas internal energy per unit volume,

$$\dot{E}_C = n_e n_p \Lambda(T) = \frac{n_t^2}{4}\Lambda(T) = \left(\frac{\bar{\rho}_e}{2\mu m_p}\right)^2 \Lambda(T), \tag{A13}$$

where

$$\Lambda(T) = \frac{2.18\times 10^{-18}}{T^{0.6826}} + 2.706\times 10^{-47} T^{2.976}\ {\rm erg\,cm^3/s} \tag{A14}$$

(see Mathews & Bregman 1978, CO01). We thus obtain

$$\tau_{cool} = \frac{6\mu m_p k}{\bar{\rho}_e}\frac{T}{\Lambda(T)}. \tag{A15}$$

A2.3 Stellar physics

The gas recycled by the evolving stellar population is given by equation (A4). The modulating (normalized) kernel is given by

$$W_*(t) = R_* \times \frac{\delta_* - 1}{\tau_0}\left(\frac{\tau_0}{t+\tau_0}\right)^{\delta_*}, \tag{A16}$$

where we adopt $R_* = 0.3$, $\delta_* = 1.36$, $\tau_0 = 10^8$yr; thus, a fraction R_* of the stellar mass produced at any time step is recycled at the end to the galaxy interstellar medium. The function above is a fairly acceptable fit of the time dependent mass return rate of a simple, passively evolving stellar population, adopted in Ciotti et al. (1991) (hereafter CDPR), CO97, 01.

A2.4 MBH accretion physics

Concerning equations (A5) and (A6), we define

$$\dot{M}_{\rm Edd} \equiv \frac{L_{\rm Edd}}{\epsilon c^2}, \tag{A17}$$

where $0.001 \le \epsilon \le 0.1$ and $L_{\rm Edd}$ is given in equation (1). The Bondi accretion rate is given by

$$\dot{M}_{\rm B} = 4\pi R_{\rm B}^2 \rho_{\rm B} c_{\rm s}, \tag{A18}$$

where $R_{\rm B}$ is given by equation (5) and

$$c_{\rm s}^2 = \left(\frac{\partial p}{\partial \rho}\right)_{isot} = \frac{kT}{\mu m_p}. \tag{A19}$$

An estimate of the gas density at $R_{\rm B}$, $\rho_{\rm B}$, is obtained from equation (A9) evaluated at $r = R_{\rm B}$[4].

[4] Note that the Bondi accretion rate given by equations above becomes irrelevant when the gas is colder than the virial temperature, because the Bondi radius is then larger than the MBH radius of influence. More appropriate in this case would be to calculate the accretion rate for the conditions at the influence radius. However, for the adopted gas density profile the accretion rate will in fact remain unchanged.

A3 Feedback and gas escape

In the following two sections we describe two different kinds of *heating* that act on the galactic gas, plus the gas cooling: note that we are not counting cooling twice, because the cooling function in equation (A13) is used to determine the gas cooling time only. Thus, we determine the gas temperature at each time-step by integrating the equation for the internal energy per unit volume

$$\dot{E} = \dot{E}_{H,SN} + \dot{E}_{H,w} + \dot{E}_{H,AGN} - \dot{E}_C + \dot{E}_{ad} + 3\frac{\dot{M}_{inf}\lambda v_{esc}^2 - \dot{M}_{esc}c_{\rm s}^2}{16\pi R_{\rm e}^3}, \tag{A20}$$

where λ is a dimensionless parameter ranging from 0.25 (corresponding to virial velocity) to 1; $\dot{E}_{ad}$ describes the adiabatic cooling in case of gas escaping (Sect. A3.4), while $\dot{E}_{H,w}$ describes the energy input due to the thermalization of red-giants wind (Sect. A3.2). As a reference value we use the quantities within the half mass radius (here identified with $R_{\rm e}$) and, accordingly, the gas internal energy is given by equation (A12), while only half of the gas accretion/outflow kinetic energy is considered. In particular, in the integration of equation above we adopt a global fitting formula for the quantity $\dot{E}_{H,AGN} - \dot{E}_C$ (Sect. A3.3). From equations (A12) and (A20)

$$T(t+\Delta t) = \frac{2\mu m_p E(t+\Delta t)}{3k\bar{\rho}_e(t+\Delta t)}. \tag{A21}$$

At each time-step a check on the attained gas temperature is performed, and we force the gas temperature to remain above the minimum value $T_{min} = 10^4$ K. Energy (temperature) integration is actually the last time-step in the integration cycle. When a new interation starts, we first check if the new determined temperature is higher than the escape temperature $\eta_{\rm esc}T_{\rm vir}$. If the condition is not satisfied (i.e., $T < \eta_{\rm esc}T_{\rm vir}$), gas escape is suppressed. On the contrary, if $T \ge \eta_{\rm esc}T_{\rm vir}$, we adopt

$$\tau_{esc} \equiv \frac{2R_{\rm e}}{c_{\rm s}} \tag{A22}$$

in equation (A7).

Note that an elementary application of the Virial Theorem, coupled with the definition of escape velocity and under the assumption that the gas is distributed as the dark matter halo, would predict that its mass weighted escape temperature correspond to $\eta_{\rm esc} = 4$. However, this is certainly an upper limit, and we expect that feedback effects will be important at much lower temperatures, say $\simeq 2T_{\rm vir}$ or even less.

A3.1 SNII, SNIa, OB and red giants wind heating

We describe here the first two contributions to the gas heating in equation (A20). The supernova heating $\dot{E}_{H,SN} = \dot{E}_{II} + \dot{E}_{Ia}$ is given by the sum of SNII and SNIa energy injection. Due to the very short life-time of massive stars, the SNII heating is assumed istantaneous.

We now compute the expected number of SNII events from a new stellar mass added to the galaxy according to the first term in the r.h.s of equation (A3). Let $\dot{M}_*^+$ be the total stellar mass assembled in the unit time, without considering the successive mass losses. We adopt a Salpeter IMF distribution, with the standard low mass cut-off $M_{*,i} = 0.1M_\odot$,

while for simplicity we assume an infinite value for the upper mass:

$$\Psi = AM^{-(1+x)} = \dot{M}_*^+(x-1)M_{*,i}^{x-1}M^{-(1+x)}, \quad \text{(A23)}$$

with $x = 1.35$. The number of SNII events per unit time is just given by the number of stars with $M > M_{II} = 8M_\odot$:

$$\dot{N}_{II} = \int_{M_{II}}^{\infty} \Psi\, dM = \left(1 - \frac{1}{x}\right) \frac{\dot{M}_*^+}{M_{*,i}} \left(\frac{M_{*,i}}{M_{II}}\right)^x. \quad \text{(A24)}$$

The total energy released by the SNII per unit time is then given by $\dot{N}_{II}E_{SN}$ (where $E_{SN} = 10^{51}$erg/s), while the actual gas heating is $\eta_{SN}\dot{N}_{II}E_{SN}$, where η_{SN} is an efficiency factor. *Note that the value of the efficiency η_{SN} is highly uncertain, depending on the particular status of the ISM. In addition, in our simple formalism in the factor $\eta_{SN} >$ we also consider the energy injected by stellar winds by the massive OB stars.* In the computed models we adopt $\eta_{SN} = 0.5$.

The treatment of SNIa heating is more complicate, being caracterized by a delayed explosion with respect to the star formation episode. We adopt here the same description as in CDPR, CO97, CO01. Thus, if $\dot{N}_{Ia}dt'$ is the total number of SNIa that will explode at $t \geq t'$ as a consequence of the star formation episode at t', and $W_{Ia}(t-t')$ the normalized explosion rate, one obtains

$$\dot{E}_{Ia} = \eta_{SN}E_{SN}\int_0^t \dot{N}_{Ia}(t')W_{Ia}(t-t')dt', \quad \text{(A25)}$$

where for simplicity we adopted the same efficiency as for SNII. Following CDPR

$$W_{Ia}(t) = \frac{\delta_{Ia}-1}{\tau_{Ia}}\left(\frac{\tau_{Ia}}{t+\tau_{Ia}}\right)^{\delta_{Ia}}, \quad \text{(A26)}$$

where $\delta_{Ia} \simeq 1.4 - 1.6$ and we arbitrarily assume $\tau_{Ia} \simeq 0.5$ Gyrs.

We do not enter here in the complicate problem of the determination of the present rate and the total number of SNIa explosions in a given stellar population: in the present treatment we just assume that for each of the star formation episodes $N_{Ia} = \vartheta_{Ia}N_{II}$. The actual value of ϑ_{Ia} is fixed by (arbitrarily) requiring that the *standard solar proportion* is maintained, i.e., that SNIa provide 3/4 of the iron in the ISM, while the remaining 1/4 is provided by SNII (Renzini et al. 1993). Because each SNIa produces $\simeq$ 10 times more Iron that a SNII, then $\vartheta_{Ia} \simeq 0.3$.

Thus, the gas heating per unit volume within $R_{\rm e}$ due to SNII, stellar winds from OB stars, and SNIa, is given by

$$\dot{E}_{H,SN} = \frac{3\eta_{SN}E_{SN}(\dot{N}_{II}+\dot{N}_{Ia})}{8\pi R_{\rm e}^3}, \quad \text{(A27)}$$

Finally, thermalization of stellar winds emitted by red-giants to the stellar velocity dispersion "temperature" is an important contribution to the global energy budget of the ISM in early type galaxies (see, e.g., CDPR). Here we describe this term as

$$\dot{E}_{H,w} = \frac{9\dot{M}_{rec}v_c^2}{32\pi R_{\rm e}^3} \quad \text{(A28)}$$

i.e., we evaluate the energy input per unit volume inside $R_{\rm e}$.

Thus, the characteristic heating time due to the global energy input of the evolving stellar population is

$$\tau_{heat,SN,w} = \frac{3k\bar{\rho}_e T/2\mu m_p}{\dot{E}_{H,SN}+\dot{E}_{H,w}}. \quad \text{(A29)}$$

A3.2 Adiabatic cooling

If the gas escape condition is satisfied, the escaping gas not only carries out kinetic energy, but also decreases its internal energy in order to expand. We evaluate the cooling due to gas expansion by using the First Law of Thermodinamics. In particular, the mechanical work of expansion is given by $-pdV$. During the expansion the gas mass is conserved, so that $V = M_{gas}/\rho$ and $dV = -M_{gas}d\rho/\rho^2$. The variation of internal energy (per unit volume, as required in energy equation above) due to gas expansion is then given by $pM_{gas}d\rho/(V\rho^2) = pd\ln\rho$. Then, from $\rho \propto r(t)^{-3}$, and by assuming that the expansion velocity is given by the sound velocity, we obtain

$$\dot{E}_{ad} = -E\frac{c_{\rm s}}{R_{\rm e}} = -2\frac{E}{\tau_{esc}}, \quad \text{(A30)}$$

where we used the identity $E = 3p/2$ and as order of magnitude $r \simeq 2R_{\rm e}$. The equation above is integrated with time-splitting. No adiabatic heating is considered in case of infall, being considered as accretion of clouds.

A3.3 AGN radiative feedback

Using XSTAR (Kallman 2002) we compute the net volume heating rate $\dot{E}$ of a cosmic plasma exposed to radiation characterized by the average quasar SED adopted from SOS. Photoionization equilibrium is assumed. $\dot{E}$ depends on gas temperature T and on the ionization parameter ξ, which can be determined from equations (2) and (A9) as follows:

$$\xi \equiv \frac{L}{n(r)r^2} = \frac{3L}{\bar{\rho}_e R_{\rm e}^2}, \quad \text{(A31)}$$

where $L = \epsilon c^2\dot{M}_{BH}$ is calculated at each time-step from equation (A6). Note that from equation (A9) ξ is independent of radius (as far as the gas is optically thin).

The following furmula provides a good approximation to $\dot{E}$ (all quantities are expressed in cgs system):

$$\dot{E} = n^2(S_1 + S_2 + S_3), \quad \text{(A32)}$$

where n is the H nucleus density (in number),

$$S_1 = -3.8\times10^{-27}\sqrt{T} \quad \text{(A33)}$$

are the bremsstrahlung losses,

$$S_2 = 4.1\times10^{-35}(1.9\times10^7 - T)\,\xi \quad \text{(A34)}$$

is Compton heating (cooling), and

$$S_3 = 10^{-23}\frac{a + b\,(\xi/\xi_0)^c}{1+(\xi/\xi_0)^c} \quad \text{(A35)}$$

is the sum of photoionization heating, line and recombination continuum cooling.

$$a = -\frac{18}{e^{25(\log T-4.35)^2}} - \frac{80}{e^{5.5(\log T-5.2)^2}} - \frac{17}{e^{3.6(\log T-6.5)^2}}, \quad \text{(A36)}$$

$$b = \frac{1.7\times10^4}{T^{0.7}}, \quad \text{(A37)}$$

$$c = 1.1 - \frac{1.1}{e^{T/1.8\,10^5}} + \frac{4\times10^{15}}{T^4}, \quad \text{(A38)}$$

and finally

$$\xi_0 = \frac{1}{1.5/\sqrt{T} + 1.5\times10^{12}/\sqrt{T^5}} +$$

$$\frac{4\times10^{10}}{T^2}\left[1+\frac{80}{e^{(T-10^4)/1.5\,10^3}}\right]. \tag{A39}$$

The formula above is applicable in the temperature range $10^4 \leq T \leq 3\times10^7$ independently of the ξ value, except for $T < 2\times10^4$ when it breaks down at $\xi < 0.01$ (hydrogen becomes neutral), but then $S_1, S_2, S_3 \to 0$.

For $T > 3\times10^7$ K one can use the approximation $\dot{E} = n^2(S_1+S_2)$.